# On the Crystalline Structures of Poly(tetramethylene adipate)

**Emilie Pouget, Ahmed Almontassir, María T. Casas, and Jordi Puiggalí***

*Departament d'Enginyeria Química, Universitat Politècnica de Catalunya, Av. Diagonal 647, E-08028, Barcelona, Spain*

*Received August 29, 2002; Revised Manuscript Received November 1, 2002*

ABSTRACT: Structural analyses have been undertaken with the monoclinic and orthorhombic crystalline structures of polyester 4 6. X-ray diffraction patterns performed at 50 °C and electron diffraction patterns from single crystals, solution-grown films, and epitaxial crystallizations have been considered. Skew $CH_2$-$CH_2$−OC(O) bonds and a $P12_1/n1$ space group were postulated for the monoclinic structure (α-form). Molecular packing was optimized from electron diffraction data and a final *R* factor of 0.19 was obtained. The orthorhombic structure (*β*-form) is characterized by an extended conformation and a molecular packing similar to polyethylene. Thus, an *R* factor of 0.11 is calculated for a setting angle of 40°, taking into account the electron diffraction data. A regular folding habit is found in the lamellar surfaces of crystals belonging to the *β*-form, whereas an irregular folding habit is characteristic of the α-form.

## Introduction

Recent efforts have been focused on the study of aliphatic polyesters due to their biodegradability.[1,2] These are mainly concerned with hydroxyacids derivatives, such as poly-ϵ-caprolactone, polyglycolide, polylactide, and poly(*R*)-3-hydroxybutirate, and also on polymers derived from diols and dicarboxylic acids, like poly(tetramethylene succinate). A systematic structural investigation on this last family has not been undertaken, and consequently, there are insufficient data on these kinds of polymers. As a general trend, a practically extended molecular conformation is postulated for polymers with long polymethylene sequences,[3,4] but kink conformations based on a pair of gauche bonds with opposite signs placed on the diol or the dicarbonilyc units have also been proposed for some ethylene glycol, succinic, and adipic derivatives.[5−7] Energy calculations on some of these polymers have also been carried out in order to determine their molecular packing. In this way, an *a* glide plane has usually been assumed for relating the chain segments that belong to the unit cell.[7] However, the structural refinement recently carried out with polyesters 4 4,[8] 6 10,[9] and 12 10[10] demonstrated the existence of an *n* diagonal glide plane, which on the other hand seems to have some peculiar repercussions on the lamellar folding surfaces. The main purpose of this work is to insist into the crystalline structure of polyester 4 6 due to the interesting results previously reported.

Lamellar crystals with large dimensions and well-developed morphologies have been obtained and studied by Minke and Blackwell.[11,12] In addition, these authors have demonstrated that polyester 4 6 exhibits polymorphism: the α-form characterized by a monoclinic unit cell with parameters $a = 6.73$ Å, $b = 7.94$ Å, $c = 14.2$ Å, and $\beta = 45.5°$ and the *β*-form with an orthorhombic unit cell of $a = 5.06$ Å, $b = 7.35$ Å, and $c = 14.7$ Å. The value of the chain axis parameter for the α-form indicates that the molecular chain was axially compressed. Chain distortion was proposed to take place in the diacid section, and particularly gauche conformations were postulated for the $C(O)CH_2$−$CH_2CH_2$ bonds.

The *β*-form is mainly observed in solution-grown single crystals, but appears as a minority component in the films and fibers prepared from the melt state. *hk*0 diffraction patterns from epitaxially crystallized samples revealed a continuos streaking on all layer lines, other than on the equator, where discrete spots were observed. This fact was attributed to disorder along the axial direction in a manner similar to that of the nematic phase of a liquid crystal.

## Experimental Section

Polyester 4 6 was synthesized from adipic acid using an excess of 1,4-butanenediol (molar ratio 2.2/1) by thermal polycondensation in a vacuum at 180 °C with titanium butoxide as a catalyst (yield 75%). An intrinsic viscosity of 0.91 dL/g was measured in dichloroacetic acid at 25 °C.

Isothermal crystallizations were carried out in the 30−40 °C range from dilute solutions (0.01% w/v) in *n*-butanol. The crystals were recovered from mother liqueur by centrifugation, repeatedly washed with *n*-butanol, and deposited on carbon-coated grids, which were shadowed with Pt−carbon at an angle of 15° for bright field observations. Polymer decoration was achieved by evaporating polyethylene onto the surface of single crystals as described by Wittmann and Lotz.[13]

Spherulites from formic acid solutions (5%, *w*/*v*) were obtained by evaporation. A Carl Zeiss Standard GFL optical microscope and a first-order red tint plate were used to determine the sign of spherulite birefringence under cross-polarization. Spherulites were covered with a thin carbon film, floated off on water, and picked up on copper grips for electron microscopy observations.

Oriented ultrathin samples suitable for electron diffraction were also obtained by stroking of concentrated formic acid solutions or by epitaxial crystallization on benzoic acid following the technique previously used for polyesters.[14] Highly birefringent zones of these films were selected under the polarizing microscope and transferred onto EM grids.

A Philips TECNAI 10 electron microscope was used and operated at 80 and 100 kV for bright field and electron diffraction modes, respectively. Selected area electron diffraction patterns were recorded on Kodak Tri-X films. The patterns were internally calibrated with gold ($d_{111} = 0.235$ nm). Electron diffraction patterns were digitised and the intensity of reflections determined by means of the ELD program.[15] This also allows one to estimate the intensity of saturated reflections by a shape-fitting procedure. If a reflection is saturated, the central part of the spot is useless. However, the tail is not saturated, so that part can be compared to the tail of a Gaussian type function. A curve-fitting algorithm is used by

10.1021/ma0214052 CCC: $25.00 
Published on Web 01/14/2003

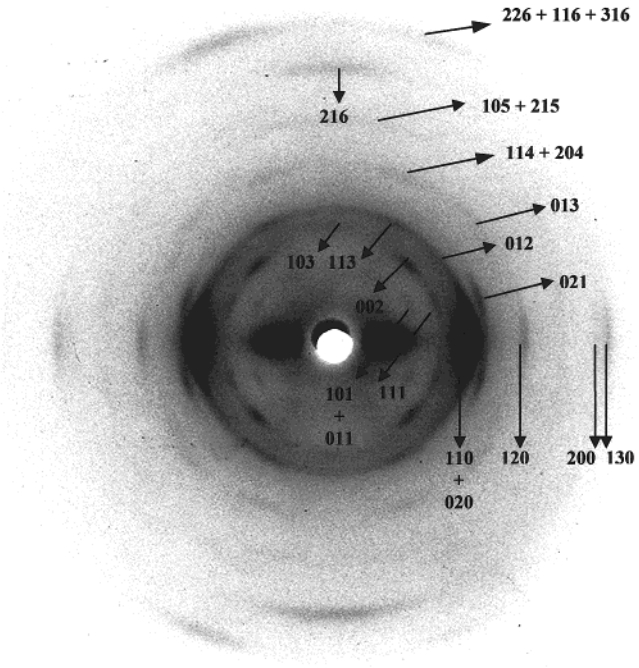


**Figure 1.** X-ray diffraction pattern of a polyester 4 6 fiber showing labeling of the main reflections. The pattern was registered at 50 °C.

the program to estimate what the reflection intensity would have been if the spot had not been saturated.

X-ray diagrams were recorded under vacuum at room temperature, with calcite as a calibration standard. A modified Statton camera (W. R. Warhus, Wilmington, DE) with Ni–copper radiation of wavelength 0.1542 nm was used. Fibers were prepared from the melt and annealed under stress at 50 °C. Patterns were also registered at 50 °C by using a temperature-controller chamber provided by the manufacturer.

Structural modeling was carried out by using the diffraction software package of the Cerius[2] (Biosym/Molecular Simulations Inc.)[16] computer program. All these calculations were run on a Silicon Graphics Indigo Workstation.

## Results and Discussion

X-ray fiber patterns of polyester 4 6 usually correspond to a mixture of the α and $\beta$ structures.[12] The latter is the minoritary structure and can be distinguished by the strong 020 equatorial reflection that appears at 3.66 Å. However, a pattern of a pure α form could be obtained (Figure 1) when an stretched fiber is maintained at 50 °C. This is in agreement with previous calorimetric studies[11] that show different melting peaks at 47 and 58 °C for the $\beta$ and α forms, respectively. The X-ray fiber diffraction pattern shows the weak 101, 103, and 105 reflections that exclude the $P12_1/a1$ space group usually postulated for this kind of aliphatic polyesters. In fact, systematic absences are only detected for the $h00$ ($h$ = odd), $0k0$ ($k$ = odd), and $h0l$ ($h + l$ = odd) reflections, suggesting an space group with a diagonal glide plane ($P12_1/n1$), as recently found for polyesters 4 4,[8] 6 10,[9] and 12 10.[10] The 002 reflection defines a $cc^*$ angle of 45.5° and a fiber repeat of 14.2 Å that are in agreement with the reported unit cell parameters and indicate a departure from an extended conformation.

**Solution-Grown Single Crystals.** Crystallizations from dilute *n*-butanol solutions preferentially render the diamond-shaped crystals of the $\beta$-form together with a few hexagonal crystals of the α-form (Figure 2a), as previously reported by Minke and Blackwell.[12] Both

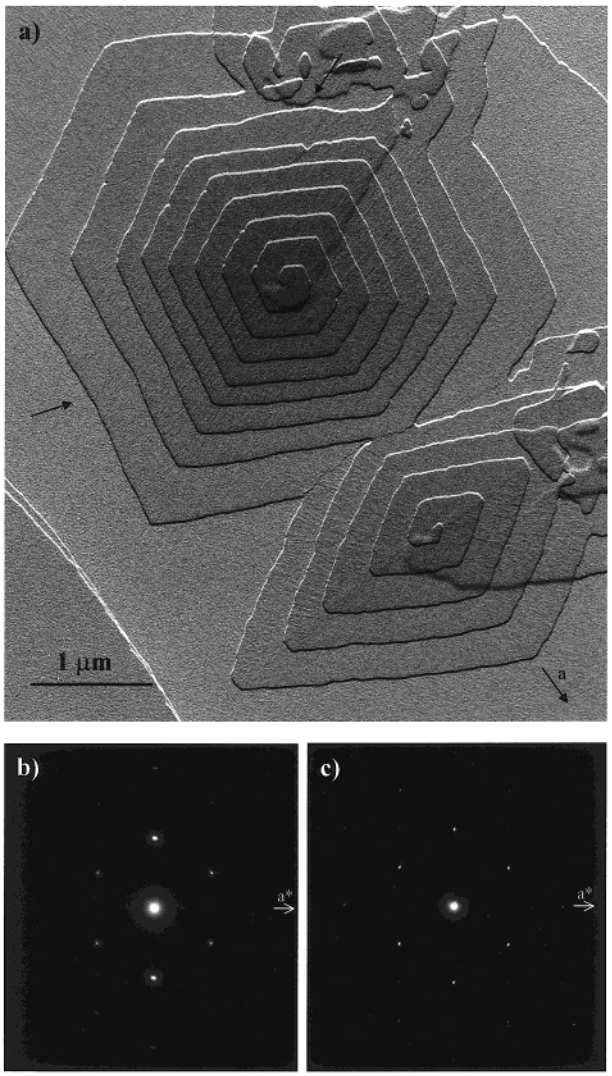


**Figure 2.** (a) Electron micrograph showing the hexagonal and lozenge morphologies of the two crystalline structures of polyester 4 6. Both crystals have an spiral growth until impingement. The direction of the *a* crystallographic axis for the $\beta$-form is indicated by arrows as well as some distinctive irregular front edges in the crystals of the α-form. (b) Electron diffraction pattern of the α-form. (c) Electron diffraction pattern of the $\beta$-form.

kind of crystals usually appears as spiral growths, with the thickness of each layer being close to 60 Å. The electron diffraction patterns of both forms can be easily differentiated due to the substantial increase on the relative intensity of the 020 and 040 reflections for the α-form (Figure 2, parts b and c). In addition, $hk0$ patterns are always observed, indicating that in both crystallographic structures the molecular chains are perpendicularly oriented with respect to the crystal basal plane.

Diamond-shaped crystals show striations at right angles to the (110) growth faces, highlighting a sectorization of crystals with the two diagonals as boundaries. These kind of corrugations have recently been described for some polyesters[17] and nylons[18] and interpreted as a consequence of a chain axis shift between neighboring chains along the growing planes. In any case, this feature contrasts with the characteristic bands observed in the lozenge crystals of polyethylene and polyester 10 16,[4] which are associated with the collapse of hollow pyramidal structures during sedimentation.

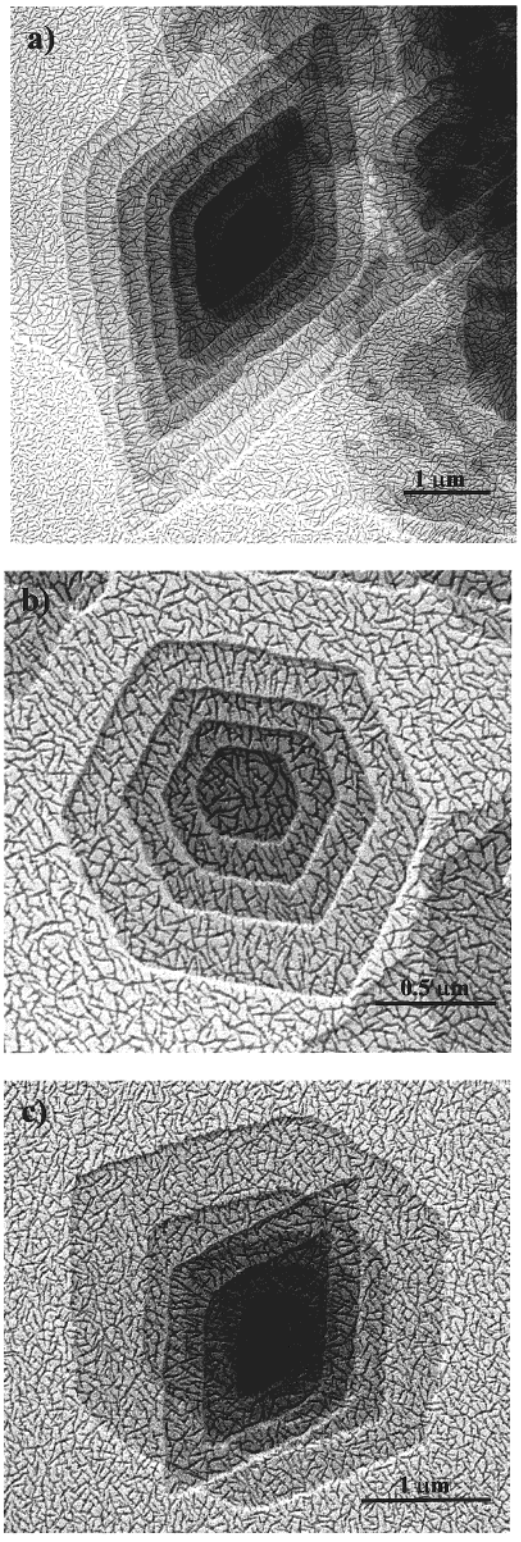


**Figure 3.** Polyethylene decoration of lamellar crystals of the $\beta$-form (a) and the α-form (b). In some cases, an epitaxial crystallization is produced between both kind of crystals (c).

Striations are also detected in the hexagonal crystals. These preferentially appear in the more developed {110} sectors and are oriented practically parallel to the *a* crystallographic axis. These extinction bands may indicate the non planar nature of the crystals, a fact that can also explain the observation of an *hk*0 electron diffraction pattern for a monoclinic unit cell with $\beta \neq 90°$.

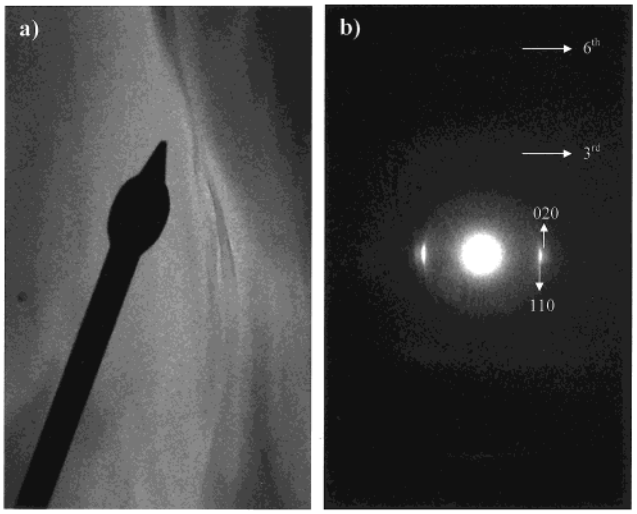


**Figure 4.** (a) Oriented film prepared by stroking a concentrated formic acid solution of polyester 4 6. (b) Electron diffraction pattern of a selected area of the indicated film. The chain axis is vertical and coincides with the direction of stroking.

Polyethylene decoration (Figure 3) shows irregular and regular folding habits on the lamellar surfaces of crystals corresponding to the α- and $\beta$-forms, respectively. Thus, polyethylene rods are perpendicular oriented to the (110) growth faces of lozenge crystals (Figure 3a), indicating that molecular folds are established along these planes. On the contrary, as shown in Figure 3b, rods are randomly oriented on the surface of the multilayered hexagonal crystals. In fact, the degree of perfection of these crystals is lower than the lozenge ones, so it is possible that folds were established along different directions in a given sector. Note for example in Figure 2a the not-well-defined front edges indicated by arrows. Figure 3c allows us to compare the different decoration effects on crystals prepared under the same conditions. Note also that the lozenge crystals are epitaxially grown over the hexagonal ones keeping the same orientation of the *a* and *b* crystallographic axes. The picture shows also the different angle between the (110) growth faces for the lozenge (120°) and the hexagonal crystals (108°).

**Structure of the $\beta$-Form.** Diffraction patterns of oriented films obtained from concentrated formic acids solutions show that the $\beta$-form develops preferentially. In this way, it is possible to select a diffracting area corresponding exclusively to this crystallographic form by means of electron microscopy (Figure 4). The pattern shows the intense 110 and 020 reflections at 4.16 and 3.66 Å and broad and weak streaks for the nonequatorial reflections. Similar results were reported from quenched films after melt pressing[11] or by epitaxial crystallization on trioxane.[12] Thus, all experimental evidences indicate that the $\beta$-form is characterized by a slippage along the molecular chain axis between neighboring molecules. The third and sixth layer lines are the most intense and define a chain periodicity of 14.7 Å, which is the expected value for an extended conformation.

Negative birefringent spherulites could also be observed when the formic acid solution is evaporated without stretching (Figure 5a). The spherulites have a ringed texture (with a ring spacing close to 2 $\mu$m), as clearly shown in the electron micrographs (Figure 5b),

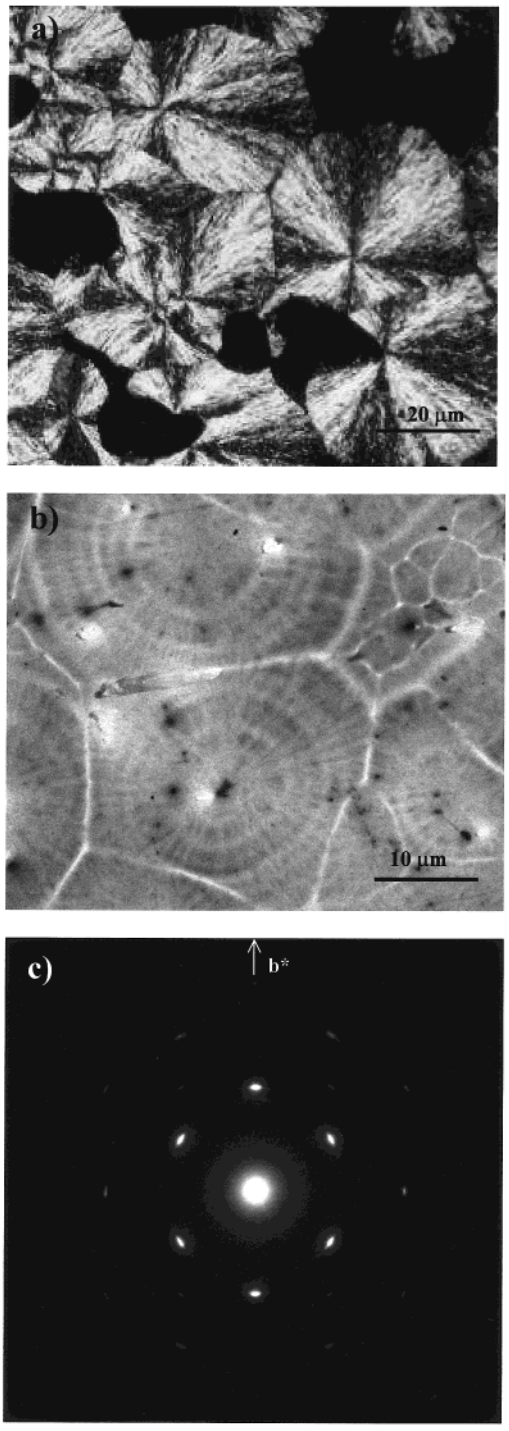


**Figure 5.** (a) Optical micrograph of negative birefringent spherulites of polyester 4 6 obtained by evaporation of formic acid solutions. Note the characteristic maltese cross. (b) Electron micrograph of the indicated spherulites showing a ringed texture. (c) Electron diffraction pattern of a polyester 4 6 spherulitic film. *b** appears to be aligned along the spherulitic radius.

and a diameter close to 30 $\mu$m. Banded spherulites are commonly observed in crystalline polymers and are generally attributed to a lamellar twisting in the direction of radial growth. Electron diffraction patterns taken from spherulites correspond to the $\beta$-form, in agreement with the structure mainly observed in stretched films. Correlation between bright-field micrographs and diffraction patterns indicates that the radial growth direction coincides with the *b* crystallographic axis. In some cases, well-defined diffraction patterns were obtained from small areas of the spherulitic film (Figure 5c). Note that the observed samples may correspond to very thin films that remain adhered to the carbon film. The electron difractogram has a 2*mm* symmetry and is similar to the patterns of polyethylene and polyesters with an orthorhombic unit cell and a fully extended conformation. Systematic absences are only noted for *h*00 and 0*h*0 with *h* and $k \neq 2n$, indicating the existence of symmetry elements as $2_1$ screw axes and/or glide planes that relate the two chain segments that belong to the unit cell.

**Table 1. Observed ($F_0$) and Calculated ($F_c$) Electron Beam Structure Factors for the $\beta$-form of Polyester 4 6**

| *hkl* | *d*(obsd) (Å) | *m*[a] | $F_o$[b] | $F_c$ $B^c = 0$ | $F_c$ $B^c = 5$ |
|---|---|---|---|---|---|
| 110 | 4.16 | 2 | 24.0 | 24.0 | 24.0 |
| 020 | 3.67 | 1 | 25.0 | 22.1 | 21.8 |
| 200 | 2.53 | 1 | 12.0 | 9.4 | 8.3 |
| 120 | 2.97 | 2 | 6.8 | 7.9 | 7.4 |
| 210 | 2.40 | 2 | 3.4 | 4.4 | 3.8 |
| 130 | 2.21 | 2 | 10.0 | 10.0 | 8.4 |
| 220 | 2.08 | 2 | 7.9 | 7.8 | 6.3 |
| 230 | 1.76 | 2 | 2.6 | 5.8 | 4.2 |
| 040 | 1.83 | 1 | 5.9 | 7.2 | 5.4 |
| | | | | $R_f = 0.11$ | $R_f = 0.12$ |

[a] Multiplicity. [b] All equivalent spots have a similar intensity. [c] Temperature factor in Å$^2$. [d] R factor calculated as $(\sum m|F_o - F_c|)/\sum mF_o$.

Structural analysis was performed in order to obtain only the optimum setting angle, since the indicated disorder makes unfeasible the determination of the space group symmetry. Electron diffraction patterns were simulated with the Cerius[2] program, assuming both an extended conformation and a *pgg* planar group. The setting angle, measured between the *a* axis and the *ab* projection of a C═O bond, was varied in steps of 5° from 0 to 90°. An optimum *R* factor was attained with a setting angle in the 40 ± 5° range. The value of 0.11 reported in Table 1 for a setting angle of 40° appears significantly better, according to the test of Hamilton,[19] than the *R* factors higher than 0.15 that are attained when the angles are lower or higher than 35 and 45°, respectively. A worse agreement between experimental and calculated intensities was found when an isotropic thermal factor of 5 Å$^2$ was considered. Although this fact appears physically unrealistic, it is in agreement with electron diffraction calculations that take only into account the kinematics approximations. Figure 6 shows the optimized packing and the simulated electron diffraction pattern for the $\beta$ structure of polyester 4 6.

**Structure of the α-Form.** Epitaxial crystallizations were performed in order to improve the electron diffraction data obtained from solution-grown single crystals. Better results were attained when benzoic acid was used as a substrate. Note the orientation of the polyester growth after dissolution of the substrate (Figure 7a). The electron diffraction pattern (Figure 7b) of a part of the film correspond to the [001] zone axis, indicating a (110) type contact plane. Furthermore, the *b* crystal axis of polyester 4 6 is oriented parallel to the preferential growth direction of substrate, which means the direction of the applied temperature gradient for its oriented crystallization. The pattern shows very weak reflections, such as 210, which intensity could not be measured in the previous patterns from single crystals.

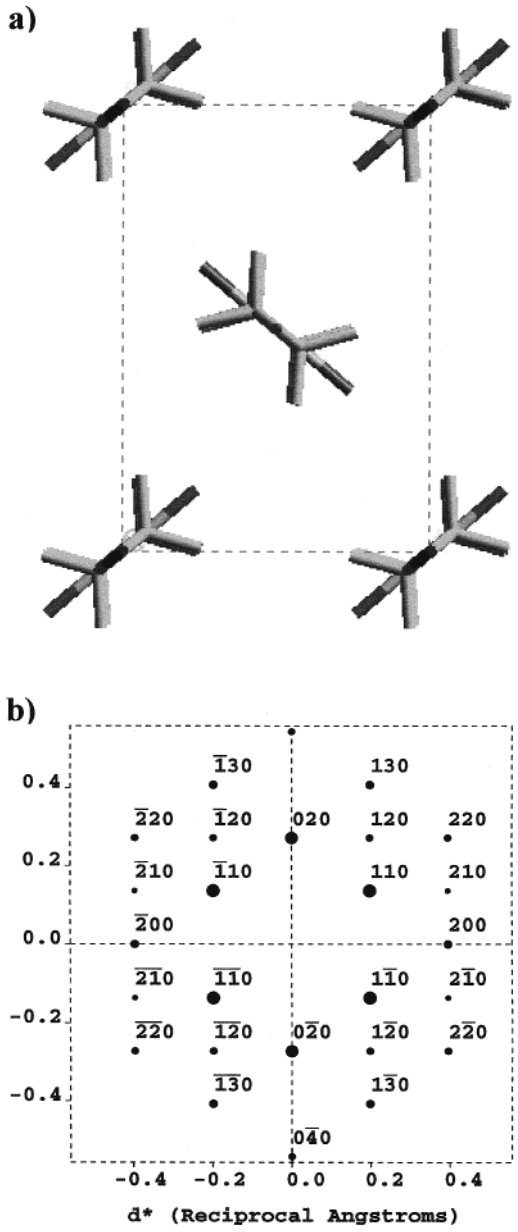


**Figure 6.** (a) *ab* projection of the refined unit cell for the $\beta$-form of polyester 4 6. Color code: hydrogen and carbon, gray; oxygen, black. (b) Calculated *hk*0 electron diffractogram for the refined packing of the $\beta$-form.

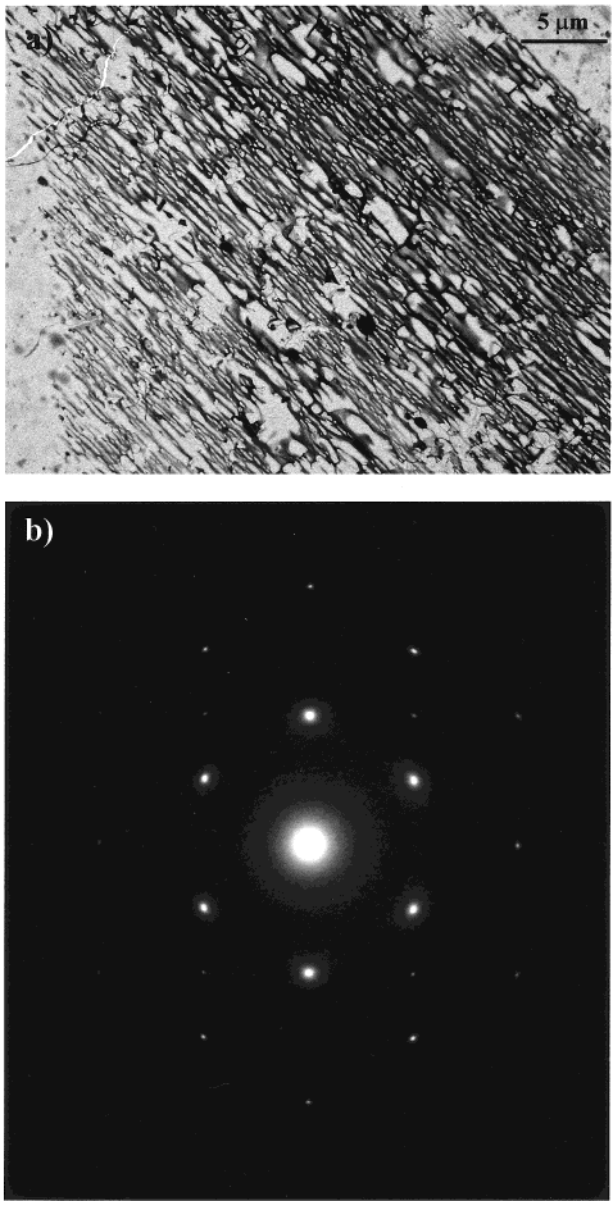


**Figure 7.** (a) Electron micrograph of the epitaxial grown of polyester 4 6 induced by a benzoic acid substrate. (b) Electron diffraction pattern of a selected area of the above indicated film.

Structural modeling has been performed assuming a molecular symmetry characterized by an inversion center in the middle of both diol and dicarbonylic units of polyester 4 6. This is the only symmetry element that may be kept when molecular chains are distorted from an extended conformation with a 2/*m* molecular symmetry.

Quantum mechanical calculations on small diamides,[20] diketones,[21] or diesters[22] indicate that the C(O)-$CH_2$−$CH_2CH_2$ torsion angles tend to adopt a gauche conformation when the dicarbonylic unit has a low number of methylene groups, as it is the case of adipate derivatives. However, the experimental chain axis repeat (14.2 Å) is much higher than that expected one (13.6 Å) for standard bond distances, bond angles, and a kink conformation based on the indicated gauche bonds (Scheme 1, $\psi_2 = -\psi_2' = 60°$). Four molecular conformations have been considered in this work for the structural refinement. Only the $\varphi_1$, $\psi_1$, and $\psi_2$ torsion

**Scheme 1**

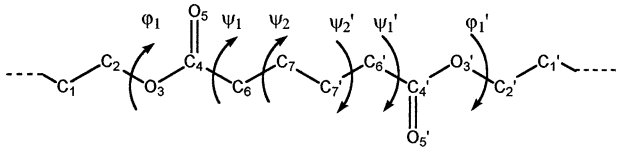


angles (Scheme 1) were allowed to deviate from 180° to fit the measured chain repeat. Figure 8 shows the variation of the chain repeat with the torsion angle for the four studied models: I ($\psi_2 = -\psi_2'$), II ($\psi_1 = -\psi_1'$), III ($\varphi_1 = -\varphi_1'$), and IV ($\varphi_1 = -\varphi_1' = -\psi_1 = \psi_1'$). Note that the indicated angles must be in the 120−108° range for a chain repeat of 14.2 Å, which seems energetically disfavored for the single $CH_2$−$CH_2$ bond of model I.

Structures were built assuming the $P12_1/n1$ space group deduced from X-ray fiber diffraction data. The asymmetric unit consists of a half molecule, which was placed in the unit cell according to the crystallographic rules. Thus, the inversion center that coincides with the

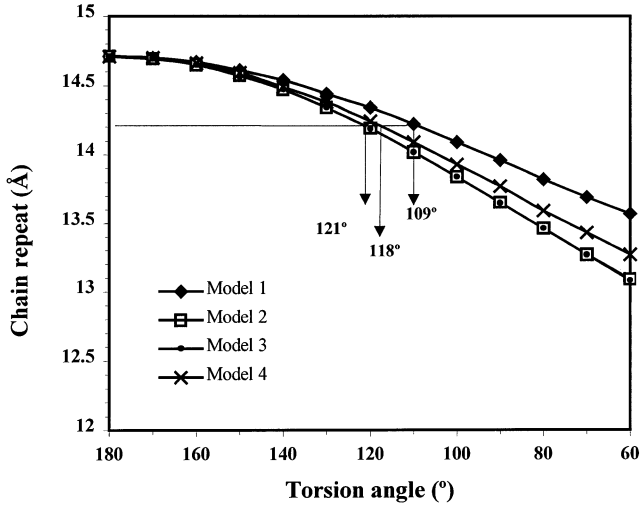


**Figure 8.** Plot of the chain repeat length vs the torsion angle variable for the four studied models. Angles corresponding to the experimental repeat are labeled.

**Table 2. Observed ($F_0$) and Calculated ($F_c$) Electron Beam Structure Factors for the α-Form of Polyester 4 6**

| *hkl* | *d*(obsd) (Å) | *m*[a] | $F_o$[b] | $F_c$ $B^c = 0$ | $F_c$ $B^c = 5$ |
|---|---|---|---|---|---|
| 110 | 4.11 | 2 | 42.5 | 42.5 | 42.5 |
| 020 | 3.97 | 1 | 54.0 | 47.2 | 47.2 |
| 120 | 3.06 | 2 | 7.0 | 6.4 | 6.0 |
| 200 | 2.40 | 1 | 9.4 | 13.6 | 11.8 |
| 130 | 2.32 | 2 | 17.6 | 16.9 | 14.4 |
| 210 | 2.30 | 2 | 1.5 | 0.4 | 0.3 |
| 220 | 2.05 | 2 | 7.0 | 9.0 | 7.3 |
| 040 | 1.99 | 1 | 12.5 | 10.7 | 8.4 |
| 140 | 1.83 | 2 | 2.5 | 4.6 | 3.4 |
| 230 | 1.78 | 2 | 1.4 | 0.6 | 0.4 |
| 240 | 1.53 | 2 | 4.2 | 5.6 | 3.6 |
| | | | | $R_f = 0.19$[d] | $R_f = 0.19$[d] |

[a] Multiplicity. [b] All equivalent spots have a similar intensity. [c] Temperature factor in Å$^2$. [d] *R* factor calculated as $(\sum m|F_o - F_c|)/\sum mF_o$.

middle of the diol unit is placed at the unit cell origin. Note that the molecular shift between neighboring molecules is defined by the space group symmetry, and consequently, only the setting angle could be refined against the diffraction data. In a similar way, as explained before, it was defined as the angle between the *a* axis and the *ab* projection of a C═O bond. It has been varied in steps of 10° from 0 to 180°, simulating both the X-ray and the electron diffraction patterns. The first ones were qualitatively compared to the experimental fiber pattern and used to discard the more divergent structures. The second ones were used to quantify the *R* factors allowing a small variation (± 5°) of the setting angles for the previously selected structures. The best agreement was obtained with model III, where only the C(O)O−$CH_2CH_2$ bonds of the diol unit were allowed to deviate from a trans conformation. These kind of skew bonds have been reported for the related polyester derived from ethylene glycol and adipic acid.[23] In summary, model III was the only one that could attain both a good agreement between the simulated and experimental X-ray diffraction patterns and an *R* factor lower than 0.3 from the analysis of the electron diffraction data. The optimum setting angle was found in the −10 ± 5° range. The calculated electron diffraction pattern showed as the main discrepancy a low intensity for the 020 reflection with

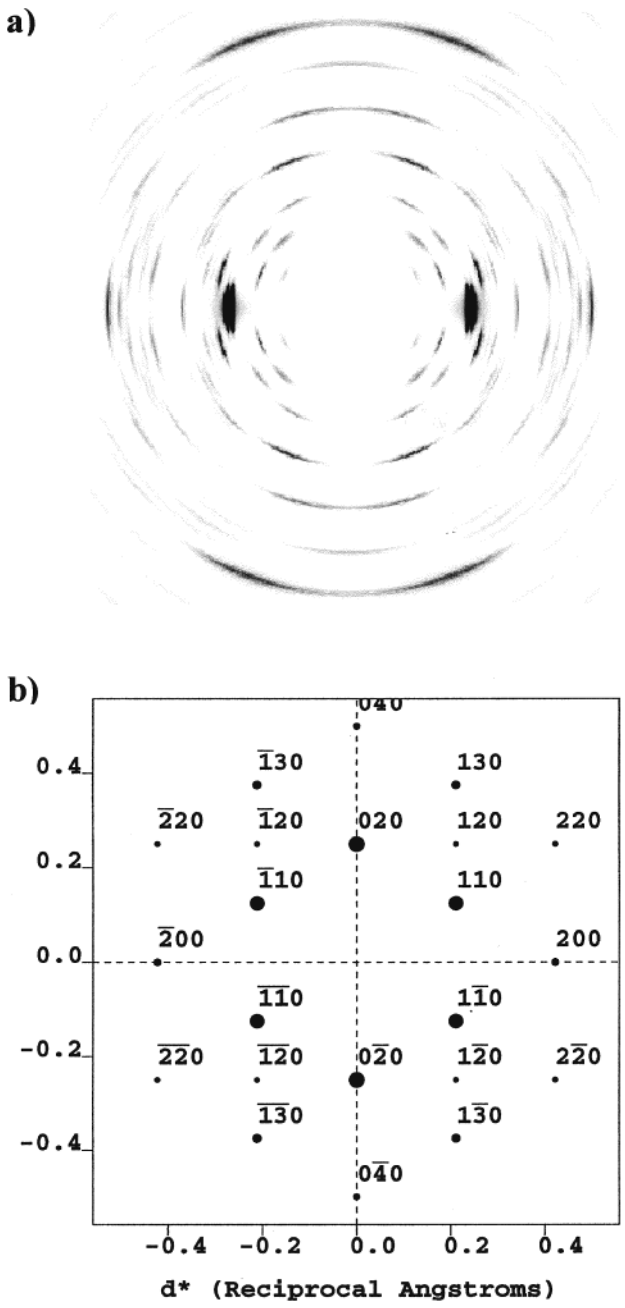


**Figure 9.** Simulated X-ray fiber diffraction pattern (a) and *hk*0 electron diffraction pattern (b) of the refined structure for the α-form of polyester 4 6.

respect to the calculated one for the 110 reflection. This feature can be easily improved by allowing a small chain distortion that mainly affects the $\psi_2$ torsional angle, which means the orientation in the unit cell of the methylene carbons of the dicarbonylic unit. Thus, values for $\varphi_1$, $\psi_1$, and $\psi_2$ of +122, −175, and +165°, respectively, give a significantly improved *R* factor of 0.19 (Table 2) for the setting angle of −10°, which still remains the best one. Simulations using isotropic thermal parameters did not improve the final *R* factor. The calculated X-ray and electron diffraction patterns of the final structure are shown in Figure 9, whereas the fractional coordinates of the symmetric unit are summarized in Table 3.

The molecular packing of the α-form of polyester 4 6 (Figure 10) has two interesting features:

**Table 3. Fractional Coordinates for the α-form of Polyester 4 6**

| atom | *x* | *y* | *z* |
|---|---|---|---|
| $C_1$ | −0.0155 | −0.0383 | 0.0529 |
| $C_2$ | 0.0247 | −0.0927 | 0.1104 |
| $O_3$ | −0.1110 | −0.0427 | 0.2456 |
| $C_4$ | 0.0432 | −0.0341 | 0.2721 |
| $O_5$ | 0.3025 | −0.0616 | 0.1785 |
| $C_6$ | −0.1069 | 0.0101 | 0.4105 |
| $C_7$ | 0.0835 | 0.0000 | 0.4290 |

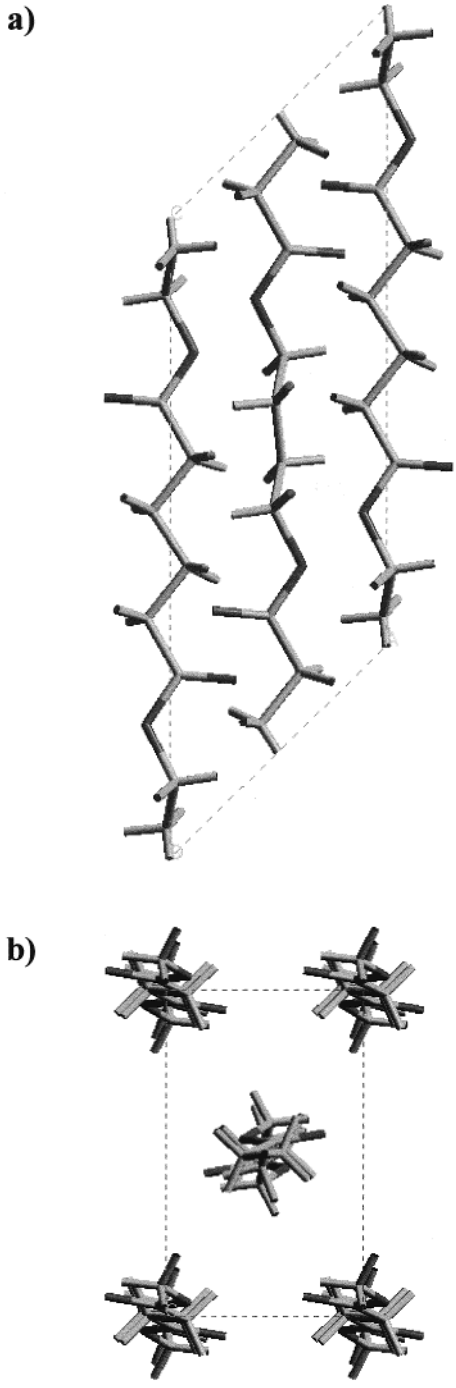


**Figure 10.** Views of the proposed structure of the α-form of polyester 4 6: (a) view parallel to the *b*-axis direction, (b) View parallel to the *c*-axis direction. Color code: hydrogen and carbon, gray; oxygen, black.

(a) The distances between the chain axes of neighboring chains along the [100] and [110] directions are practically identical (4.80 and 4.64 Å, respectively).

(b) A chain axis shift close to four bonds exists between neighboring molecules along the [100] direction, whereas a shift of eight bonds (or minus four bonds) is found along the [110] direction.

Thus, it may be inferred that adjacent folds along both the [100] and [110] directions involve the same kind of chemical groups. Note also, that these must be the ester groups due to the reduced number of methylene groups (four in both diol and dicarbonylic units) and the large shift (four bonds) between adjacent molecules. This observation contrasts with the differences on the lamellar surface recently deduced for other polyesters[10,11] with an *n* glide plane symmetry.

## Conclusions

Lamellar crystals of the *β*-form are characterized by a lozenge morphology and the establishment of molecular folds along the (110) growth faces. In addition, a chain-axis shift between neighboring molecules could be deduced from the X-ray and electron diffraction patterns, a feature that may be related with the corrugations observed on the lamellar surfaces. Molecules with an extended conformation pack according to an orthorhombic unit cell and a setting angle similar to that found in polyethylene. Ringed spherulites corresponding to the *β*-form could be obtained by evaporation of formic acid solutions, with the *b* crystallographic axis parallel oriented to the spherulitic radius.

Structural analysis of the monoclinic structure suggests a conformation based on a pair of skew bonds of opposite sign in the diol unit, and a $P12_1/n1$ space group. Hexagonal lamellar crystals of the α-form show more irregular front edges than those of the *β*-form and also an irregular folding habit. The molecular packing suggests that ester groups must be involved in the folds that take place through both [100] and [010] directions.

**Acknowledgment.** This research has been supported by the CICYT (MAT2000-0995).

## References and Notes

(1) Huang, S. J. In *Encyclopedia of Polymer Science and Engineering*; Wiley-Interscience: New York, 1985; Vol. 2, p 20.
(2) Fujimaki, T. *Polym. Degrad. Stab.* **1997**, *30*, 7403.
(3) Fuller, C. S. J. *Am. Chem. Soc.* **1939**, *61*, 2575.
(4) Kanamoto, T.; Tanaka, K. *J. Polym. Sci., Part A-2* **1971**, *9*, 2043.
(5) Ueda, A. S.; Chatani, Y.; Tadokoro, H. *Polym. J.* **1991**, *2*, 387.
(6) Aylwin, P. A.; Boyd, R. H. *Polymer* **1984**, *25*, 323.
(7) Liau, W. B.; Boyd, R. H. *Macromolecules* **1990**, *23*, 1531.
(8) Ichikawa, Y.; Kondo, H.; Igarashi, Y.; Noguchi, K.; Okuyama, K.; Washiyama, J. *Polymer* **2000**, *41*, 4719.
(9) Armelin, E.; Casas, M. T.; Puiggalí, J. *Polymer* **2001**, *42*, 5695.
(10) Armelin, E.; Almontassir, A.; Franco, L.; Puiggalí, J. *Macromolecules* **2002,** *35*, 3630.
(11) Minke, R.; Blacwell, J. *J. Macromol. Sci., Phys.* **1979**, *B16*, 407.
(12) Minke, R.; Blacwell, J. *J. Macromol. Sci., Phys.* **1980**, *B18*, 233.
(13) Wittmann, J. C.; Lotz, B. *J. Polym. Sci., Part B: Polym. Phys.* **1985**, *23*, 205.
(14) Wittman, J. C.; Lotz, B. *J. Polym. Sci., Polym. Phys. Ed.* **1981**, *19*, 1853.
(15) ELD[2.1], Quantitative Electron Diffraction. Calidris: Manhemsvägen 4, Sollentuna, Sweden.
(16) Cerius[2]. Molecular Simulations Inc.: Burlington, MA.
(17) Furuhashi, Y.; Iwata, T.; Sikorski, P.; Atkins, E.; Doi, Y. *Macromolecules* **2000**, *33*, 9423.
(18) Bermudez, M.; León, S.; Alemán, C.; Muñoz-Guerra, S. *J. Polym. Sci., Polym. Chem. Ed.* **2000**, *38*, 41.

(19) Hamilton, W. C. *Acta Crystallogr.* **1965**, *18*, 502.
(20) Navarro, E.; Alemán, C.; Puiggalí, J. *J. Am. Chem. Soc.* **1995**, *117*, 7307.
(21) Alemán, C.; Navarro, E.; Puiggalí, J. *J. Phys. Chem.* **1996**, *100*, 16131.
(22) Alemán, C.; Puiggalí, J. *J. Org. Chem.* **1997**, *62*, 3076.
(23) Turner-Jones, A.; Bunn, C. W. *Acta Crystallogr.* **1962**, *15*, 105.

MA0214052